

Micro-machined Vibrating Ring Gyroscope Testing

Vasilii Kirnos, Aleksander Vagachev
Yaroslavl State University
Yaroslavl, Russia
v.kirnos@uniyar.ac.ru, aleksvagachev@yandex.ru

Oleg Morozov
Institute of Physics and Technology
of Russian Academy of Sciences, Yaroslavl Branch
Yaroslavl, Russia
moleg1967@yandex.ru

Abstract—Resonance frequency and Q-value are the main characteristics of micro-machined vibrating ring gyroscopes. Asymmetry can cause mismatch of gyroscope made of single crystal silicon. This defect can lead to a large frequency consumption of normal mode of operation. To solve this problem, measurements must be made to diagnose the quality of the vibration ring supplied. This article describes the structure of the installation for measuring ring parameters.

I. INTRODUCTION

Since the 1960s, scientific and technical work began in the field of development of miniature sensors and actuating devices of various purposes based on silicon. Research on the creation of special materials and technologies of microelectronics has made it possible to develop designs on a single crystal. A wide range of these sensors are classified as micro-electromechanical systems (MEMS).

MEMS, in particular gyroscopes and accelerometers, belong to the class of inertial sensors, the range of which is very wide. Since the 1990s, they have are used in medicine and the civil industry - automotive, robotics, etc. [1]–[4],

Subsequently, micro-machined instruments have been used in military equipment and so far the demand for MEMS continues to grow. At the moment, the demand for MEMS is very large: from airbags and anti-lock automobile devices to small inertial navigation systems integrated with satellite navigation systems, which provide determination of orientation and navigation parameters of aircraft, surface and underwater vehicles, ground vehicles. The active development of micro-machined technologies, expansion of the field of application, a large volume of carried out research allowed to significantly increase the volume of the world market of MEMS and in 2017 to reach 21 billion dollars. Also, the accuracy characteristics were significantly improved, the instability of the zero signal reached the level of 0.1... 10 degrees per hour. [5], [6]

Among the Russian enterprises and institutes working on the creation of MEMS, it is necessary to mention: JSC Concern of CNI "Electric Appliance", N.E. Bauman's MG TU, OJSC "Gyrooptika," branch of FSUE "CENKI" - "NII PM of the Institute of Electronic Research," Among the foreign development firms are known: "Murata Manufacturing Co., Ltd. (Japan), "Honeywell, Inc." (United States), Analog Devices, Inc. (USA), British Aerospace Systems and Equipment (BASE) (UK), Silicon Sensing Systems Ltd. (England), "MT-Mirosystems CO., Ltd." (China). In general, the creation of micro-machined gyroscopes in the Russian Federation is at the stage of development of prototypes and small-scale production.

In order to solve the problem of improving the characteristics of the micro-machined vibrating ring gyroscope (Fig. 1), it was necessary to carry out a thorough analysis of the gyroscope design, analyse the technical solutions and use mathematical modelling. Parameters characterizing the accuracy and other characteristics of the gyroscope were analysed.

One parameter characterizing instrument accuracy is wave pattern drift in the start. To reduce wave pattern drift, it is necessary to minimize energy loss in the oscillating system. These losses arise because of the mechanical tension and constructive defects arising at production of a sensitive element (the sensitive element is a ring with the elastic supporting crossing points and windings which are raised dust on its surface), leading to reduction of its good quality. Increasing the accuracy of the micro-machined vibrating ring gyroscope prevents the reduction of only one error from producing the desired result. An integrated approach to the problem was thus needed.

In order to solve the problem of improving the characteristics of the ring micro-machined generator, it was necessary to carry out a thorough analysis of the gyroscope design, analyse the technical solutions and use mathematical modelling. Parameters characterizing the accuracy and other characteristics of the gyroscope were analysed.

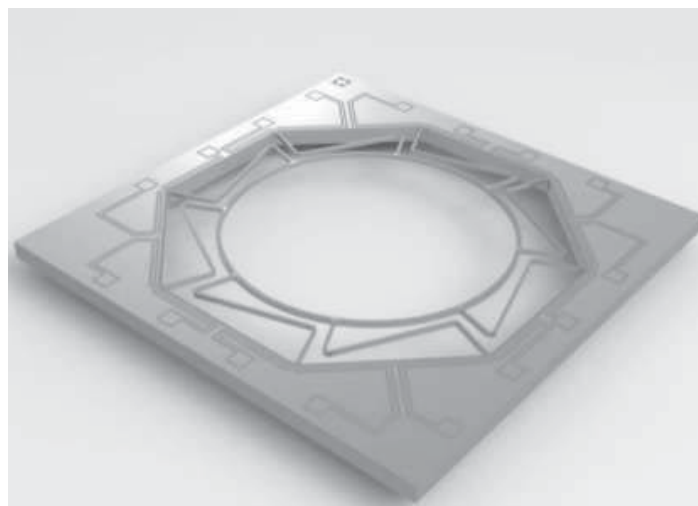


Fig. 1. The micro-machined vibrating ring gyroscope

One parameter characterizing instrument accuracy is wave pattern drift in the start. To reduce wave pattern drift, it is necessary to minimize energy loss in the oscillating system.

These losses arise because of the mechanical tension and constructive defects arising at production of a sensitive element (the sensitive element is a ring with the elastic supporting crossing points and windings which are raised dust on its surface), leading to reduction of its good quality. Increasing the accuracy of the micro-machined vibrating ring prevents the reduction of only one error from producing the desired result. An integrated approach to the problem was thus needed. [7]

This article is devoted to measurement of accuracy characteristics of micro-machined vibrating ring gyroscope under conditions of wide temperature and mechanical impacts. The relevance of the article is also related to the development of information, control, navigation and micro-system technology.

II. DESIGN AND FABRICATION OF THE RESONATOR

The manufactured resonator has a well-known construction. It is based on a 6 mm diameter silicon ring suspended on eight radially corresponding spokes. The wires are attached to a support frame with a lateral dimension of 10·10 mm² (Fig.2) The aluminum conductors located at the top of the ring and the wires form eight separated identical contours. These loops, together with a magnetic field (which is perpendicular to the plane of the ring), provide driving and sensitive transducers. Calculated natural frequency f_n of resonator operating mode is 13980 Hz

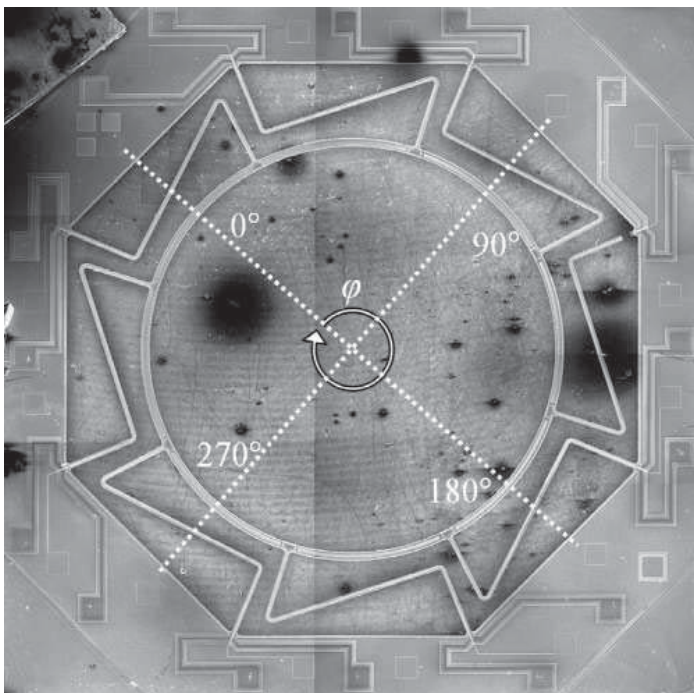


Fig. 2. Image of the fabricated resonator

The resonator is manufactured by volumetric micro-machined treatment on single-crystal silicon plate. Deep reactive ion etching of silicon is carried out with the help of own inductively coupled plasma equipment. The etching system uses time-multiplexed deep etching technology. The manufacturing process requires only three masks: two masks aligned on both sides of the wafer for silicon etching and one mask for metallization. The main manufacturing steps are

shown in Fig. 3. On a 4-inch 380- μm -single crystal silicon plate with a thermally grown oxide layer 1 μm thick on both sides of 1 and 2 masks. Then, a metal layer is thermally applied and a pattern is formed by the mask 3. The oxide formed by the mask 1 on the back side of the wafer is necessary to form a 100- μm silicon device layer by time multiplexed deep etching. To determine the structure of the resonator, an oxide with pattern 2 is required, which is then etched in the device layer by time-multiplexed deep etching. Finally, the plate is cut to release the individual resonator chips. [8]

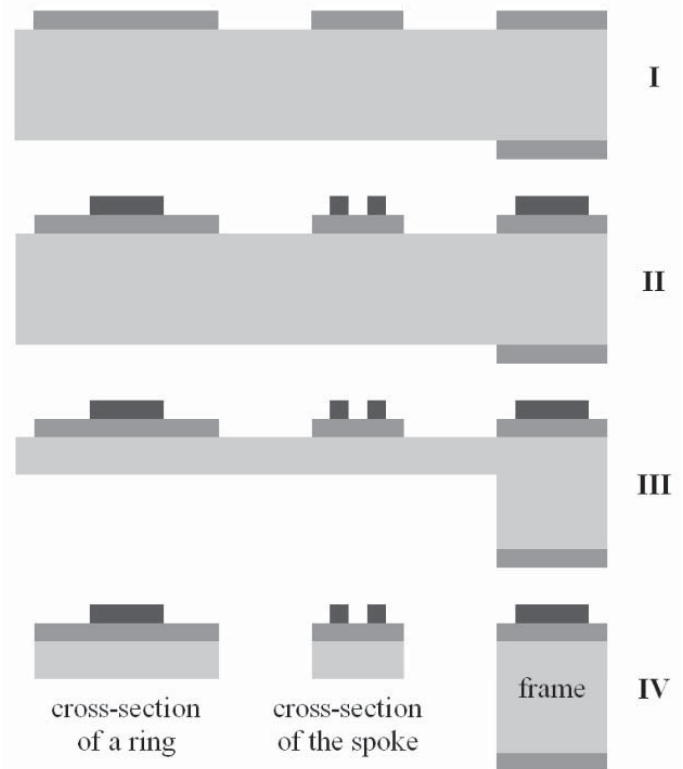


Fig. 3. Cross-section of the resonator at the main fabrication stages: I formation of the SiO₂ masking layers; II deposition of the metal conductors; III the time multiplexed deep etching from the backside of the wafer stopped by the timed end point detect method; IV through-wafer the time multiplexed deep etching.

III. MEASUREMENT TECHNIQUE

Gyroscope usually consists of base, on which service electronics of control and processing of output signal are fixed. An annular micro-machined gyroscope sensor is mounted on the upper board. Outside the gyroscope is covered with a metal jacket. In our state it is rather open and much bigger than the fabric example.

To carry out an experiment to analyse the operability of our product, a stand was assembled. This stand consists of several related parts (Fig. 4):

- The vibration ring itself, which is located on a special magnetic table. The contact pads, which are located at an angle of 180 degrees, are connected to a generator for the input action and on the other side to a device that allows to read voltage.

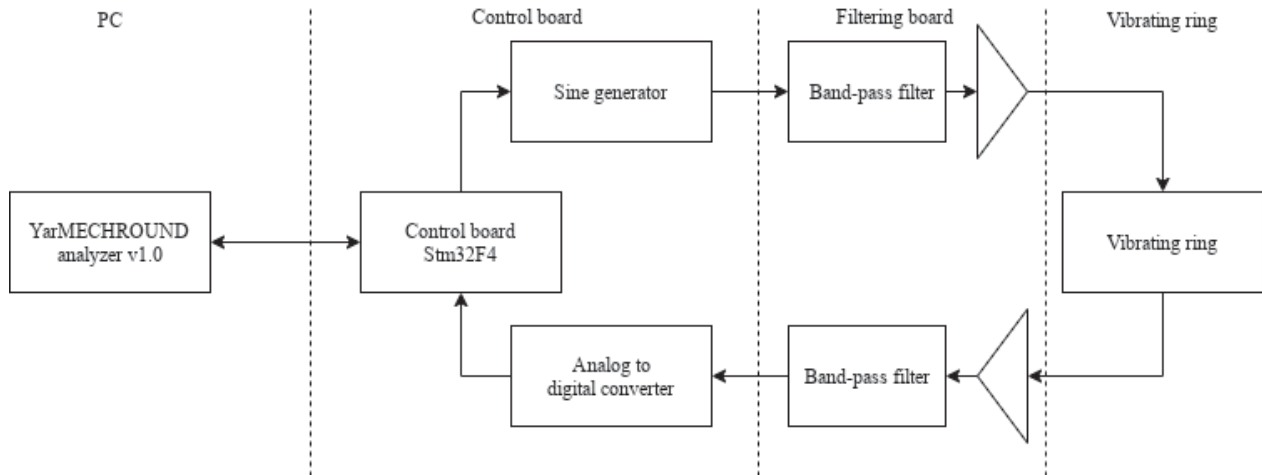


Fig. 4. state

- Filter board with the band-pass filters and amplifiers.
- Control board
- Computer with special software

A. The vibrating ring physics

The gyroscope mainly consists of an inner gimbal with inner coils, outer gimbal with outer coils, torsion bars and permanent magnets. The inner gimbal is driven by a current in inner coils to oscillate at its own resonant frequency around the torsion bars, while the outer gimbal is steady because the vibration of the inner gimbal is parallel to the torsion bar for the outer gimbal. When an angular rate is applied perpendicularly to the plane, Coriolis force at the center mass makes the oscillation of the outer gimbal and the outer-coil provides an electromotive force for the voltage detection. The device can operate at atmospheric pressure because the device has no critical parts such as narrow gaps or comb drivers, and accurate alignment of the magnetic field. [3]

The ring electrostatically vibrates into an elliptical primary bending mode with a fixed amplitude. When the device is subjected to rotation, the Coriolis force causes energy to be transferred from the primary mode to the secondary bending mode, which is located 45 degrees from the primary mode, providing a proportional increase in amplitude in the latter mode. This build-up is controlled by capacitive monitoring.

There are four drive electrodes (at 0, 90, 180, 270 degrees) and four sensor electrodes (at 45, 135, 225, and 315 degrees). The ring of the vibratory ring gyroscope has two elliptical identical bending modes (drive mode and read mode) with the same resonance frequency in different directions (45 degrees apart). Due to residual stresses during fabrication, environmental interference, or other factors, there is always frequency separation between these two modes in reality. The smaller the frequency split, the higher the sensitivity. Electromagnetic excitation and inductive sensing are used to facilitate closed loop control. The ring of the micro-machined the vibratory ring gyroscope vibrates with a fixed amplitude at the frequency of the excitation mode, applying an alternative current to the drive electrodes by means of a magnetic field. [9], [10]

The transfer function of the vibrating ring gyroscope sensitive part is:

$$H(S) = \frac{2 \cdot \xi \cdot T \cdot S}{T^2 \cdot S^2 + 2 \cdot \xi \cdot T \cdot S + 1}, \quad (1)$$

where T - constant time characterizes the oscillation system;

ξ - relative coefficient of attenuation;

S - Laplacian.

The vibrating ring gyroscope for control contours can be represented in simplified form as two interconnected resonant circuits with parameters:

f_1, f_2 - resonant frequencies along the axis of excitation and measurement, Hz;

Q_1, Q_2 - values of contour quality along excitation and measurement axis;

It will be appreciated that the transfer function is determined by the transmission coefficient.

At the sensor there are phenomena of splitting of own resonant frequency and a difference in Q-factor, i.e. inequalities of $Q_1 \neq Q_2, f_1 \neq f_2$ are carried out. Such phenomena is the result in undesirable effects when creating control contours. Lets consider the following conditions: $Q_1 = Q_2, f_1 < f_2$. This conditions will later help us with the experiment. [15], [16]

B. Hardware solution

We need to generate the sine signal, which will be later presented on the input pads of the ring. The frequency is in the range from 13.8 kHz to 14.1 kHz. The accuracy of is signal is 0.1 Hz, that's why we decided to make a solution on high speed microcontroller, which is based on the ARM architecture Stm32F4.

To discover the best solution we used board named Stm32F4-Discovery. On the board you can find the most interesting chip, named CS43L22. The CS43L22 is a highly integrated, low power stereo DAC with headphone and Class D speaker amplifiers.

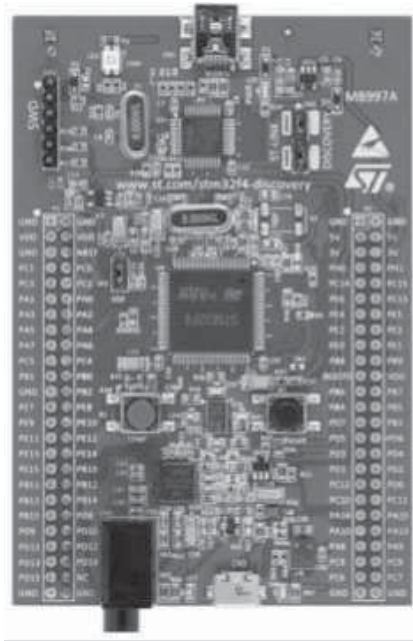


Fig. 5. Stm32F4-Discovery

Communication between the board and the computer is implemented using the UART protocol. Its velocity is quite enough to determine the amplitude value.

C. Analog filtration

During the experiments we found out that there was a high frequency noise in the resultant signal. Band-pass filters had to be added to prevent the noise between the generator output and the resonator input, as well as the resonator output and the detector input.

The suitable is active filter on an operational amplifiers. We used the Sallen and Key Filter design to design our filters. The Sallen and Key topology is an active filter design based around a single non-inverting operational amplifier and two resistors, thus creating a voltage-controlled voltage-source design with filter characteristics of, high input impedance, low output impedance and good stability, and as such allows individual Sallen-key filter sections to be cascaded together to produce much higher order filters. (Fig. 7)

The filter that skips high frequency noise is the 4th order bandpass filter Gaussian. (Fig. 6)

The electromotive force in the vibrating ring gyroscope is in the range of millivolts. We added amplifier to the filtration board and get amplification 90. The resultant board is presented on the Fig. 8

D. Pseudo-Voigt approximation

On the side of the software we have a program, which convert data from the raw data from control board to the beautiful chart with information about Q-value and resonance frequency.

A model based on a pseudo-Voigt distribution function, which is a weighted sum of a Gaussian and Lorentzian

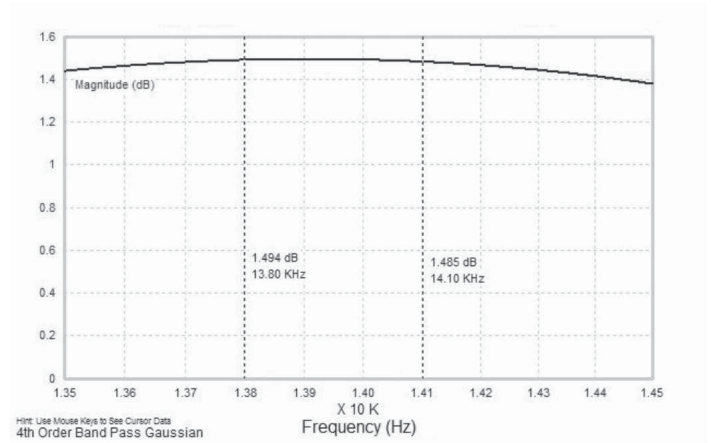


Fig. 7. Sallen and key circuit frequency response

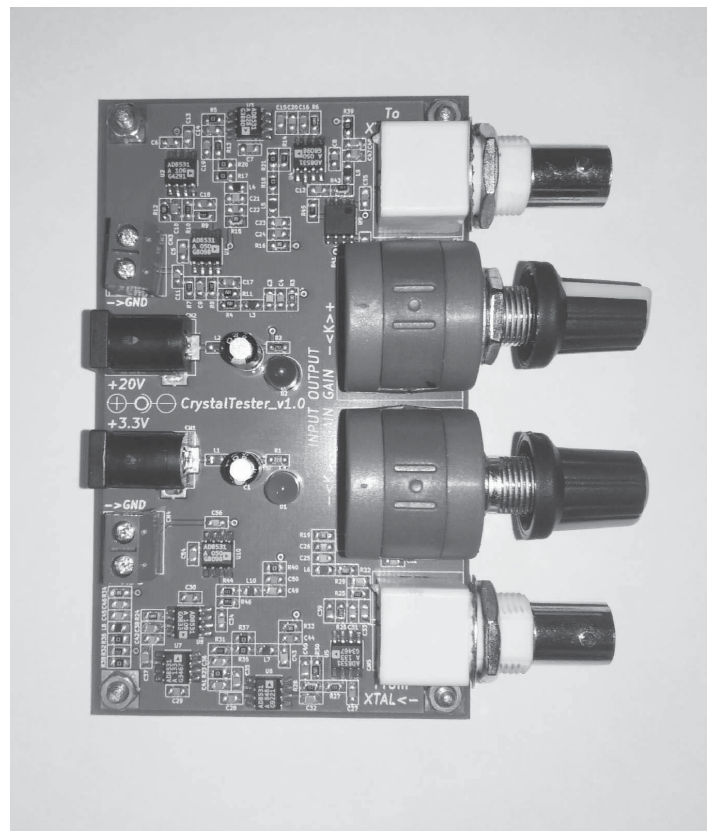


Fig. 8. Filter board

distribution function that share values for amplitude (A), center (μ) and full width at half maximum fwhm (and so have constrained values of sigma (σ) and height (maximum peak height)). A parameter fraction (α) controls the relative weight of the Gaussian and Lorentzian components, giving the full definition of

$$f(x; A, \mu, \sigma, \alpha) = \frac{(1 - \alpha)A}{\sigma_g \sqrt{2\pi}} e^{-\frac{(x-\mu)^2}{2\sigma_g^2}} + \frac{\alpha A}{\pi} \left[\frac{\sigma}{(x - \mu)^2 + \sigma^2} \right] \quad (2)$$

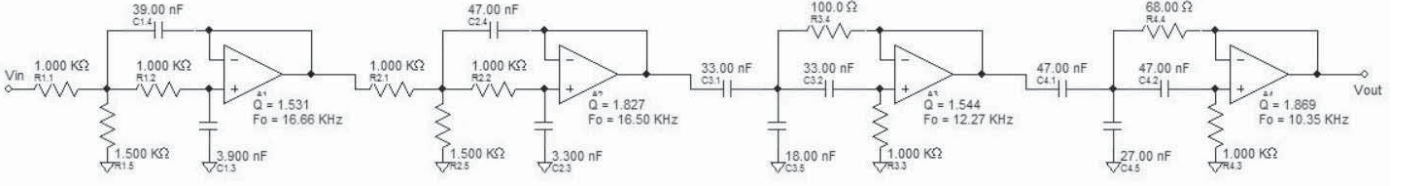


Fig. 6. 4th order bandpass filter Gaussian

IV. RESULT ANALYSE

The input signal was sinusoidal with four different amplitudes values.

Most of the resonators manufactured exhibit a frequency separation of no more than 10 Hz. However, for a precision gyroscopic operation, the relative frequency mismatch $\delta f/f_n$ should be minimized. Typically $\delta f/f_n$ must be less than $0.5/Q$, where Q is the resonator quality factor. The measured value of Q ranges from 1500 to 5000. Thus, the frequency separation should be less than 1 Hz. In order to eliminate the split, it is necessary to accurately control the location of imperfections. The resonator quality factor affects the location of the axes, which is related to the location of the defects. In our experiment, it is difficult to detect a single peak on a resonance curve when the split is below 2 Hz due to the relatively low Q value. Higher Q can be achieved by defining a dominant damping mechanism and considering various ways to reduce damping.

The gas pressure during measurement is quite low, so air damping is eliminated. This is supported by the fact that Q is reduced from 6500 in vacuum to 1500 at atmospheric pressure. A significant damping mechanism is also support loss. Ring is attached with pins to support frame. This attachment creates a path for emitting mechanical energy away from the ring.

The ring example measure is presented on Fig. 9. On the amplitudes under the a), b), c) we can see good Q -value. It means that our vibrating ring gyroscope is working in the linear mode. On the d) image the Q -value is rather smaller, we are working in non-linear mode on with the ring.

We will accept the b) solution parameter values corresponding to the parameters $Q_1 = 2531, Q_2 = Q_1 = 2531, f_1 = 13924, f_2 = f_1 + 5Hz$ in the vibrating ring gyroscope transfer function on the equation (1).

Resonance frequency splitting is 5 Hz.

We will form transfer functions for two resonance circuits with central frequencies f_1 and f_2

$\omega_1 = 2 \cdot \pi f_1$ - the vibrating ring resonance frequency along excitation axis, rad/sec;

$\omega_2 = 2 \cdot \pi f_2$ - the vibrating ring resonance frequency along measurements axis, rad/sec;

$\xi_1 = \frac{1}{2 \cdot Q_1}$ - value of relative factor of the ring attenuation along excitation axis;

$\xi_2 = \frac{1}{2 \cdot Q_2}$ - value of relative factor of the ring attenuation along measurements axis

$T_1 = \frac{1}{\omega_1}$ - transfer function time constant of the ring along excitation axis;

$T_2 = \frac{1}{\omega_2}$ - transfer function time constant along measurements axis;

The transfer function of the vibrating ring gyroscope along excitation axis is:

$$H_1(S) = \frac{2 \cdot \xi_1 \cdot T_1 \cdot S}{(T_1 \cdot S)^2 + 2 \cdot \xi_1 \cdot T_1 \cdot S + 1} \quad (3)$$

We will enter the following replacement in the equation (3) and replace the previous values:

$$H_1(S) = H_1(\omega) \text{ and } S = i \cdot \omega$$

$$H_1(\omega) = \frac{\frac{1}{Q_1 \omega_1} \cdot \omega}{-\frac{\omega^2}{\omega_1^2} + 1 + \frac{1}{Q_1 \omega_1} \cdot \omega}$$

$$H_1(\omega) = \frac{87442.72 \cdot \omega}{-2531 \cdot \omega^2 + 87442.72 \cdot \omega + 7646231812}$$

The transfer function of the vibrating ring gyroscope along measurements axis is:

$$H_2(S) = \frac{2 \cdot \xi_2 \cdot T_2 \cdot S}{(T_2 \cdot S)^2 + 2 \cdot \xi_2 \cdot T_2 \cdot S + 1} \quad (4)$$

Lets do similar transformation with the equation (4):

$$H_2(S) = H_2(\omega) \text{ and } S = i \cdot \omega$$

$$H_2(\omega) = \frac{\frac{1}{Q_2 \omega_2} \cdot \omega}{-\frac{\omega^2}{\omega_2^2} + 1 + \frac{1}{Q_2 \omega_2} \cdot \omega}$$

$$H_2(\omega) = \frac{87449 \cdot \omega}{-2531 \cdot \omega^2 + 87449 \cdot \omega + 7647330132}$$

The resulting angular velocity causes vibrations along the measurements channel.

V. CONCLUSIONS

In this article we discuss that micro-machined solid wave gyroscope is a promising technology. However, the accuracy of such a sensor is limited by geometric imperfections due to manufacturing problems. Even with modern MEMS technology, small manufacturing errors are introduced that cause frequency separation of the ring-type resonator.

Manufactured resonators have a rather large frequency separation, but with the possibility of its correction by relatively small mass cutting. The components of the correction unit were demonstrated in the subsequent processing of a ring type resonator with a comparable relative frequency divergence [10]. Modal frequency tuning first requires searching for the main axes of elasticity. The present direct measurement method

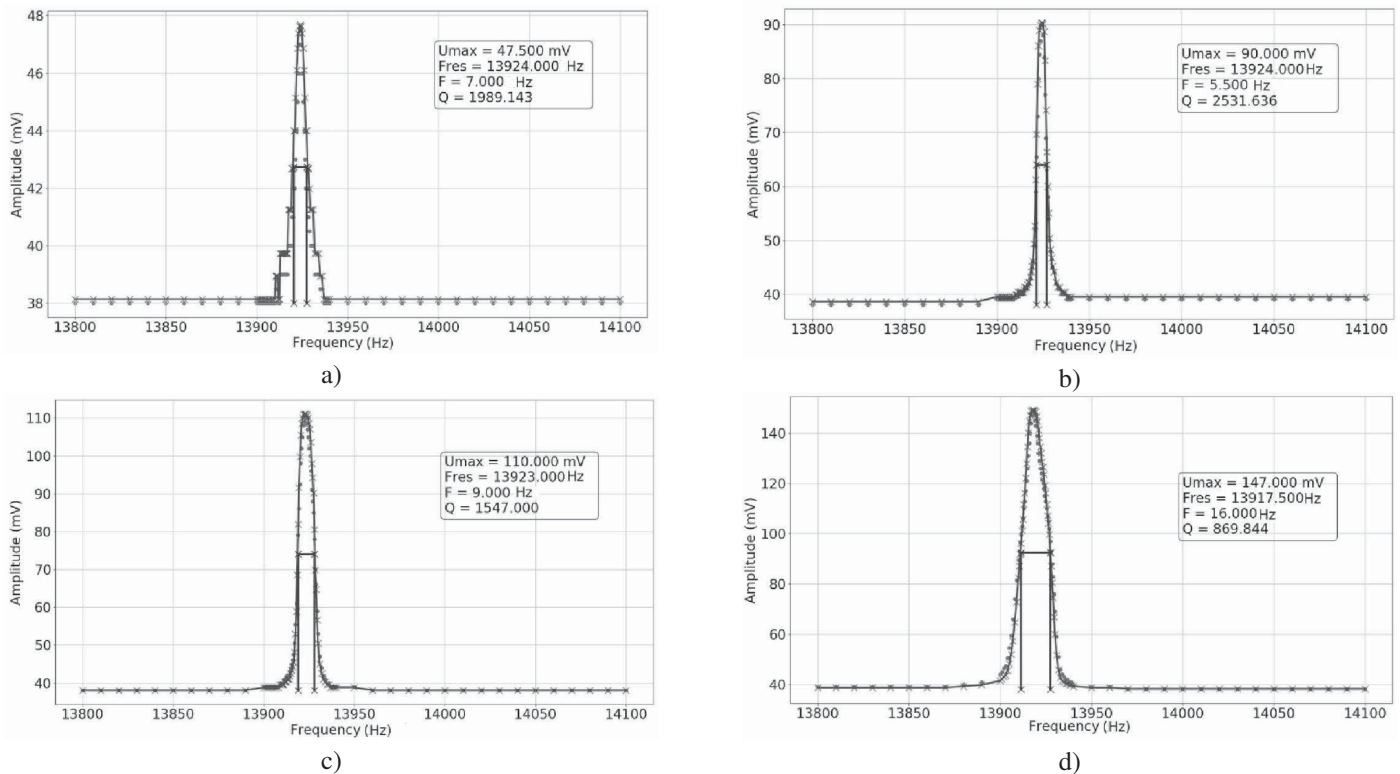


Fig. 9. Amplitude-frequency response at different input signal amplitude: a) 1V, b) 1.5V c) 2V, d) 4V.

makes it possible to quickly determine the orientation of the node element for samples with a frequency of more than 2 Hz.

Resonators with lower temperature f should be measured below room temperature. Under such conditions, the accuracy of the measurement will be increased by increasing the quality factor. This is possible due to the strong temperature dependence of thermoelastic damping as the dominant loss mechanism.

ACKNOWLEDGMENTS

Investigation was carried out under Yaroslavl Demidov State University Development Program OP-2G-07-2019.

We would like to show our gratitude to Ivan Kalistratov, Mihail Dubov, Andrey Kiselnikov, Iliia Uvarov for their pearls of wisdom with us during the course of this research, for Aleksandr Rudyi and Andrey Priorov for their organization of interaction.

REFERENCES

[1] I. Y. Xu, X. Chen, and Y. Wang, Two-mode navigation method for low-cost inertial measurement unit-based indoor pedestrian navigation, *J. Chem. Inf. Comput. Sci.*, 44(5), 2016, pp. 1840-1848
 [2] H. Huang et al., High accuracy navigation information estimation for inertial system using the multi-model EKF fusing Adams explicit formula applied to underwater gliders, *ISA Trans.* 66, 2017, pp. 414-424
 [3] D. Z. Xia, C. Yu, and L. Kong, The development of micromachined gyroscope structure and circuitry technology, *Sensors* 14(1), 2014, pp. 1394-1473
 [4] H. S. Li, H. L. Cao, and Y. F. Ni, Electrostatic stiffness correction for quadrature error in decoupled dual-mass MEMS gyroscope, *J. Micro/Nanolith. MEMS MOEMS* 13(3), 033003, 2014

[5] S. Yoon et al., Tactical grade MEMS vibrating ring gyroscope with high shock reliability", *Microelectron. Eng.* 142, 2015, pp. 22-29
 [6] F. Ayazi and K. Najafi, High aspect-ratio polysilicon micromachining technology, *Sens. Actuator A* 87(1), 2000, pp. 46-51
 [7] Liu, J.L.; Chen, D.Y.; Wang, J.B. "Fabrication and test of an electromagnetic vibrating ring gyroscope based on SOI wafer", *Journal of Electronics, China*, 2014, 31, pp. 168-173
 [8] O. Morozov, I. Uvarov, "Determination of vibration axes of the micro-machined ring resonator for the modal tuning purposes", *Proc. SPIE*, 11022, 110220W, 2019
 [9] A.M. Shkel, Type I and type II micromachined vibratory gyroscopes, *Proc. IEEE/ION Position, Location, And Navigation Symposium*, 2006, pp.586-593,
 [10] B.J. Gallacher et al., Multimodal tuning of a vibrating ring using laser ablation, *Proc. Institution of Mechanical Engineers, Part C: Journal of Mechanical Engineering Science*, 217, 2003, pp.557-576, 2003
 [11] Cao, Huiliang and Liu, Yu and Zhiwei, Kou and Zhang, Yingjie and Xingling, Shao and Gao, Jinyang and Huang, Kun and Shi, Yunbo and Tang, Jun and Shen, Chong and Liu, William, "Design, Fabrication and Experiment of Double U-Beam MEMS Vibration Ring Gyroscope", *Micromachines*. 10. 186, 2019
 [12] Zhiwei, Kou and Liu, Jun and Cao, Huiliang and Han, Ziqi and Sun, Yanan and Shi, Yunbo and Ren, Senxin and Zhang, Yingjie, "Investigation, modeling, and experiment of an MEMS S-springs vibrating ring gyroscope", *Journal of Micro/Nanolithography, MEMS, and MOEMS*, 2018
 [13] Abdul-Wahed, Ahmed and Mahmoud, Mohamed, "A Novel Multiple-Shell Vibratory Ring Gyroscope", 2015
 [14] Puchades, Ivan and Koz, Mustafa and Fuller, Lynn. "Mechanical Vibrations of Thermally Actuated Silicon Membranes", *Micromachines*, V.3, 2015, pp. 255-269
 [15] Kostornoy A., "Effect of the Gas Environment on the Characteristics of the Micro-machined Vibrating Gyroscope", *Aerospace instrument making*, V. 11, 2017, pp. 3-11
 [16] Kostornoy A., "Influence of manufacturing errors on mechanical properties and oscillations of MMG", *Aerospace instrument making*, V. 9, 2017, pp. 3-9